Annu. Rev. Fluid Mech. 1999. 31:347–84

FLUID COATING ON A FIBER

David Quéré
Laboratoire de Physique de la Matière Condensée, Collège de France, 75231 Paris Cedex 05, France

KEY WORDS: thin liquid films, wetting, boundary layers, surfactants

ABSTRACT

We discuss the thickness of the liquid layer entrained by a solid drawn out of a bath, focusing on the case where the solid is a fiber or a wire. Slow withdrawals out of a pure or a complex fluid are described as well as quick coatings. We specify the general laws of entrainment and stress the cases where the fiber curvature plays a role. We finally give an overview on the further evolution of the coated film.

1. INTRODUCTION

Fluid coating is our name for the operation of forcing a fluid to coat a solid by a movement. Painting a wall by moving a brush saturated with paint and coating a solid by drawing it out of a bath of liquid are two ways to do fluid coating. The question is often what are the parameters fixing the thickness of the deposited film and which are the entrainment laws? If this question is asked to a (scientific) audience, it receives a large variety of answers, even if one restricts it to the sign of variation of the thickness versus the velocity. A very simple argument shows that everybody is right (and thus reveals that the question is demagogic): when the velocity is zero, we find no film, since the coating results from a dynamic process; when the velocity is infinite, the same result is expected because the film has no time to develop. These rough arguments favor a picture of a nonmonotonous variation of the thickness as a function of the velocity. One of our primary aims therefore is to describe the shape of this curve. We base the following presentation on recent experimental data and try to understand the observations by the use of scaling arguments.

The pioneering works on fluid coating can be classified by the geometry of solids. The problem of a plate drawn out of an infinite reservoir (Figure 1*a*) was

0066-4189/99/0115-0347$08.00

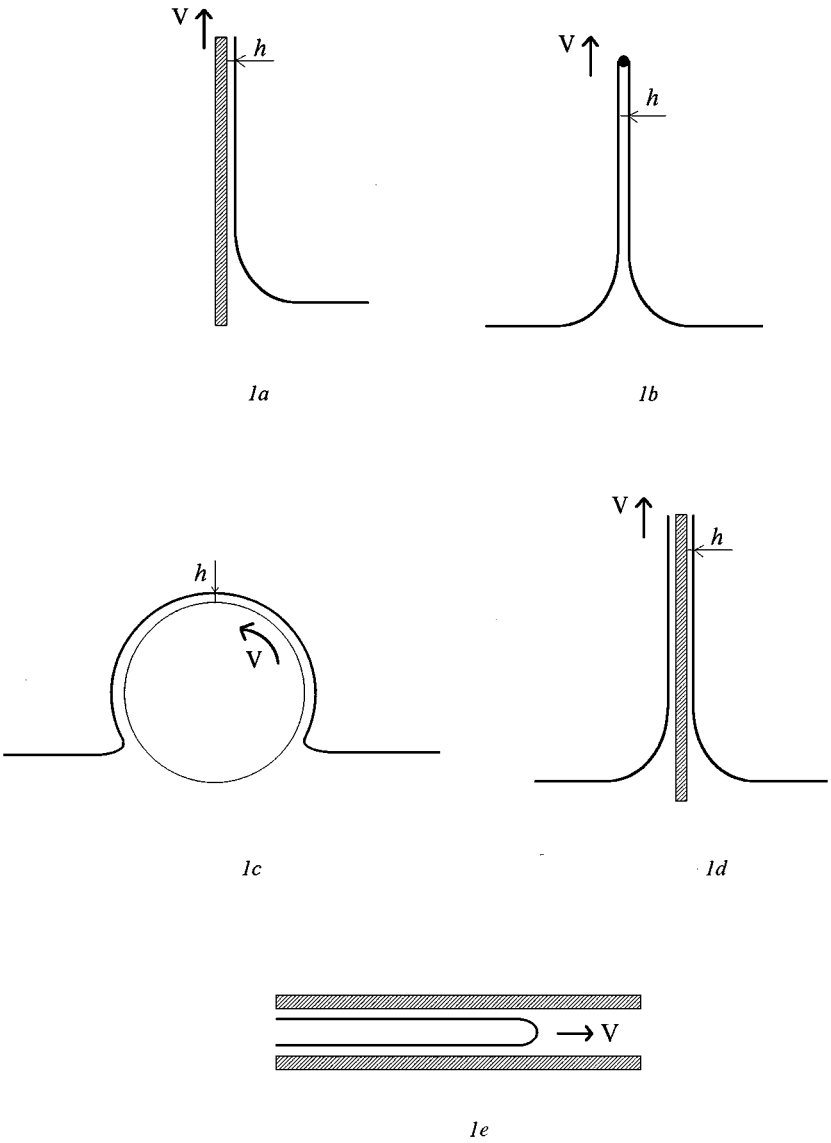

Figure 1 Various geometries for fluid coating. (*a*) Plate coating; (*b*) making of a soap film; (*c*) roll coating; (*d*) fiber coating; (*e*) coating of the inside of a tube (or a Hele-Shaw cell). In each case, a relative motion between the solid and the liquid implies the deposition of a thin liquid layer of a liquid on the solid.

the first to be experimentally studied (Goucher & Ward 1922, Morey 1940), and a famous theory was proposed in the forties by Landau & Levich (1942) and Derjaguin (1943). We summarize this LLD theory, which can be extended to all kinds of geometry. A particular case of planar withdrawal is the making of soap films from a surfactant solution (Mysels et al 1959, Mysels & Cox 1962) (Figure 1*b*).

As natural extensions, roll coating (Gatcombe 1945, Taylor 1963) (Figure 1*c*) and fiber withdrawal (Goucher & Ward 1922, White & Tallmadge 1966) (Figure 1*d*) were the topics of early investigations. Cylindrical geometry also arises in tubes; emptying of a capillary tube has been extensively studied since 1913 (Vaillant 1913, Fairbrother & Stubbs 1935, Taylor 1960, Bretherton 1961) (Figure 1*e*). A closely related problem leading to similar results is the drainage of a Hele-Shaw cell (Park & Homsy 1984, Tabeling & Libchaber 1986). Development of the pioneering works and extension to more complicated geometries are described in Ruschak's review (1985).

Here, we are mostly concerned with the case in which a solid to be fluid coated is a fiber or a wire (Figure 1*d*), which provides a convenient control parameter (the fiber radius) and allows us to isolate the effects from each other. In particular, gravity can be generally ignored if the fiber is thin enough. Besides, this case is of practical importance. Just after they are made, glass and polymeric fibers are lubricated with a liquid to prevent them from breaking during further operations. Since fibers are often used for reinforcing composites, the function of the coating may also be to provide compatibility and the desired degree of bonding with the ceramic or polymer matrix. Practically, the coating is generally achieved by drawing the fiber at high velocities (on the order of 10 m/s) out of a complex liquid (often an emulsion).

Other techniques, often described in technical reviews, can be used for more specific purposes. Freeze coating (or hot dipping), for example, consists of passing a cold wire through a globule of molten metal (Arridge & Heywood 1967). The control parameter is mainly the dipping time τ_i, which typically ranges between 1 ms and 1 s (Carreker 1963, Kornmann et al 1978). Since a thin layer of metal freezes onto the wire surface, the film thickness first increases with τ_i (Bubnov et al 1994) up to the point where the wire and the bath have the same temperature, after which it decreases. When coming out of the bath, the wire entrains molten metal, and the coating thickness finally depends on both freezing and viscous drag (Xiao et al 1994). Practically, steel wires can be coated with aluminium (Kornmann et al 1983) or polymer (Akter & Hashmi 1997) for protection against corrosion, or with copper (Brelin & Kornmann 1990) for improving the mechanical properties. As a variation on freeze coating, consider a traditional way of making candles by drawing a wick out of molten wax! Another way to achieve continuous thin films on fibers is

Figure 2 Industrial device for lubrication of glass fibers. Fibers are quickly drawn downwards and pass through a layer of a liquid coating a roll partially immersed in liquid. (Courtesy of Saint-Gobain Recherche.)

chemical vapor deposition, which provides the advantages of high purity and applicability to oxides, carbides, metals, etc. Furthermore, it eliminates the need to use a liquid phase and is well adapted to the achievement of very thin (successive) layers. A description of this technique together with an abundant bibliography can be found in a report by Lackey et al (1991).

Here, we restrict our analysis to fluid coating by using a Newtonian solution, which corresponds to many practical situations. Figure 2 presents a device for glass fiber lubrication, which combines roll and fiber coating; a roll immersed in an aqueous solution turns at a velocity of about 10 cm/s, so that it is constantly coated with a layer of liquid through which series of fibers pass at high speed (typically 30 m/s). The velocity is directed downwards since the fibers are drawn from an oven just above the lubrication stage.

One of the aims of this report is to connect the academic case (slow withdrawal from a pure liquid) with practical applications. After a presentation of the LLD theory, we discuss different causes of deviation (in order of increasing complexity): (i) gravity and effects related to the solid-liquid interface, at small velocity; (ii) influence of inertia on quick withdrawals; (iii) effects related to the liquid-air interface for coating with a complex fluid (a soapy water or an emulsion).

The different regimes are illustrated by experimental results, generally obtained by using a film balance (Figure 3) devised for this purpose (de Ryck &

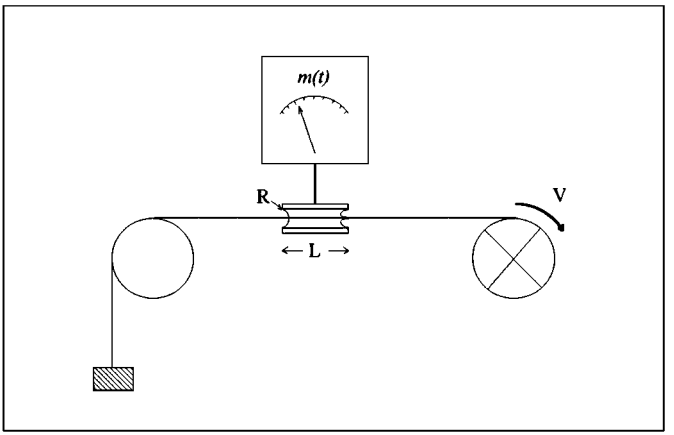

Figure 3 Film balance for measuring the film thickness entrained by a wire drawn out of a bath (of radius R and length L).

Quéré 1994). The liquid bath is a drop trapped inside a horizontal Teflon tube through which a fiber passes. The mass *m* of this drop is recorded as a function of time *t*. The entrainment is found to be stationary in most cases; as the fiber moves, the mass of the reservoir decreases linearly with time, from which the (constant) film thickness can be easily deduced. But since the measurements are done while depositing the film, this device also appears to be well adapted to unstationary entrainments; we present two examples of such behaviors.

2. SLOW AND PURE COATINGS: THE VISCOCAPILLARY REGIME

2.1 *The Goucher Picture*

In their pioneering work, Goucher & Ward (1922) identified the key parameters of the problem: if the solid is drawn slowly, the liquid layer will be thin (since it is zero when the velocity is zero, where the possible existence of a microscopic wetting film is neglected). Thus, the main roles are played by the interfaces. The solid-liquid interface is essential because the boundary condition at this interface is responsible for the liquid entrainment. Because of the liquid viscosity, the liquid near the solid must move at the same velocity as the solid (and thus comes out with it). At the same time, the motion of the solid provokes a deformation of the liquid-air interface, what the surface tension opposes. Thus, viscous and capillary forces play antagonist roles, and it is natural to consider as a key parameter the ratio of these forces. It is the so-called capillary number, which

is computed by

$$\mathrm{Ca} = \frac{\eta \mathrm{V}}{\gamma}, \tag{1}$$

where η and γ are the liquid viscosity and surface tension, respectively, and V is the coating velocity. Thus, it is expected that the film thickness can be expressed as

$$h = \ell \mathrm{f}(\mathrm{Ca}), \tag{2}$$

where ℓ is some static length, which should depend on the geometry of the solid; i.e. the capillary length for a large solid (a plate or a roll) and its radius for a fiber or a tube thinner than the capillary length. Goucher and Ward also obtained experimental data by coating metallic wires with melted beeswax and weighing them after solidification. They found that f(Ca) is an increasing function close to linearity.

2.2 *The LLD Theory*

The first (correct) determination of the function f(Ca) in Equation 2 was the theory developed by Landau, Levich, and Derjaguin (LLD theory). We summarize it by using scaling arguments. The description is based on Figure 4, drawn for the fiber case.

The region where the film forms is called the dynamic meniscus, with a thickness of order h and length λ. In this region, a flow takes place because of the Laplace pressure Δp caused by the curvature of the film: for small thickness

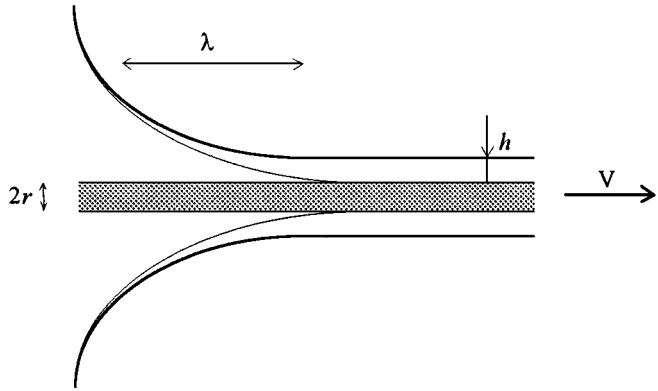

Figure 4 The LLD picture. At low speed, the top of the static meniscus is slightly deformed in a dynamic meniscus (of length λ) where the film forms.

($h \ll r$), Δp equals γ/r. If inertia can be neglected, the viscous force balances the pressure gradient along the dynamic meniscus, which is written as

$$\frac{\eta V}{h^2} \sim \frac{1}{\lambda}\frac{\gamma}{r}. \tag{3}$$

In the latter equation, λ is unknown. Some authors have proposed to make it constant (equal to the fiber radius), but this statement is not correct. One guesses that λ varies for example with the velocity. The LLD theory proposed to determine λ by matching the static meniscus with the dynamic meniscus. The matching is done by balancing the Laplace pressure, which is zero in the static meniscus if r is smaller than the capillary length (James 1974, White & Tallmadge 1965a), but incorporates two terms of opposite signs in the dynamic meniscus: one caused by the curvature of the fiber and one relative to the second derivative of the profile. Thus, the matching dimensionally is written as

$$\frac{\gamma}{r+h} - \frac{\gamma h}{\lambda^2} \sim 0. \tag{4}$$

For thin films ($h \ll r$), it yields

$$\lambda \sim \sqrt{hr}. \tag{5}$$

This simple relation appears to be very general. The length of the dynamic meniscus is the geometric mean of the two lengths of the problem (namely the thickness and the radius). Equation 5 allows us to eliminate λ in Equation 3, which leads to power laws for the film thickness and for the length of the dynamic meniscus. One finds:

$$h \sim r\mathrm{Ca}^{\frac{2}{3}} \tag{6a}$$

$$\lambda \sim r\mathrm{Ca}^{\frac{1}{3}}. \tag{6b}$$

The careful calculation derived from the LLD theory is an asymptotic matching that provides the numerical coefficient in Equation 6a (Levich 1962, Derjaguin & Levi 1964). The exact LLD law is written

$$h = 1.34r\mathrm{Ca}^{\frac{2}{3}}. \tag{7}$$

Equation 7 is sometimes referred to as the Bretherton law, since Bretherton (1991) showed that it gives the thickness of the film left behind a drop moving inside a capillary tube of inner radius r. It also gives the thickness of the film remaining at low capillary number on the walls of a Hele-Shaw cell (of spacing $2r$) emptied by a nonviscous fluid (Park & Homsy 1984). The special case in

which the fluid driving out the liquid has a nonnegligible viscosity was studied by Schwartz et al (1986). Then the film thickness should increase from the LLD value to $2^{2/3}$ (about 1.6) times the LLD value when the ratio of the surrounding fluid viscosity to the liquid one increases from zero to infinity.

2.3 *The White & Tallmadge Correction*

Equation 7 is derived for small capillary number (it is supposed that $h \ll r$, which implies $\mathrm{Ca} \ll 1$). As Ca increases, r must be replaced by $r + h$ in Equations 3 and 5 and thus in Equations 6 and 7. The entrainment law becomes (White & Tallmadge 1966)

$$h = \frac{1.34 r \mathrm{Ca}^{\frac{2}{3}}}{1 - 1.34 \mathrm{Ca}^{\frac{2}{3}}}. \tag{8}$$

The latter expression diverges for $\mathrm{Ca} = 0.64$. At this point, the gradient of pressure between the film and the reservoir vanishes. In the absence of gravity, the reservoir is fully entrained by the fiber.

In Figure 5, the measured thickness divided by the wire radius is displayed as a function of the capillary number for various wires and viscous silicone oils (de Ryck & Quéré 1996). Equation 8 is drawn in the same plot and fits quite well with the experimental data. As long as the thickness is much smaller than the radius, the LLD equation is followed; then the capillary divergence predicted by White and Tallmadge can be observed. Thus, for a model system (smooth fibers, wetting viscous liquids, and slow withdrawal), Equation 8 is obeyed on a wide range of capillary numbers. The film thickness results from a balance between the viscous forces, which are responsible for the existence of a macroscopic film, and the capillary forces, which tend to make it as thin as possible. Therefore, the visco-capillary regime concerns slow fluid coating for all pure wetting fluids.

The capillary divergence predicted by Equation 8 is specific of the fibers. Conversely, a regime of capillary convergence is expected for the film remaining behind a drop in a tube (Figure 1*e*), where the obvious inequality $h < r$ must be satisfied. Indeed, it was shown by Taylor that the film thickness becomes constant ($h \sim 0.34\, r$) as the capillary number increases (Taylor 1960, Cox 1962). The crossover regime from the LLD law to the limiting value was theoretically studied by Reinelt & Saffman (1985), who took into account the particular shape of the finger of air blowing away the liquid from the tube. Of course, a similar saturation is observed when draining a Hele-Shaw cell, where h is observed to tend to be about $0.2\, r$ (with r the half-spacing of the cell) (Tabeling et al 1987).

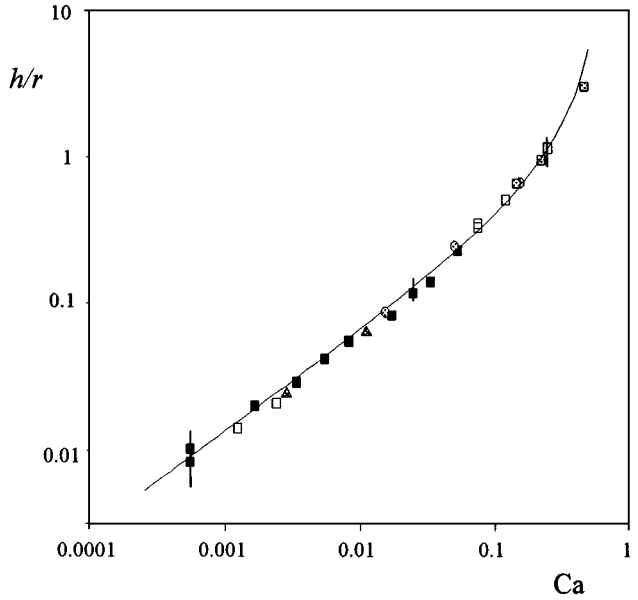

Figure 5 Slow coating of thin wires ($r = 12.5$, 63.5, or 88.5 μm) by various viscous silicone oils; the viscosities range between 20 mPa · s and 500 mPa · s and the coating velocities between 0.1 mm/s and 5 cm/s. The symbols correspond to different radii and oil viscosities, but all the data obey the WT equation (Equation 8), a generalized form of the LLD law (Equation 7).

3. DEVIATIONS FROM THE LLD LAW AT LOW VELOCITIES

Natural limitations on Equations 7 and 8 may be significant, even with the restriction to slow withdrawal out of a pure Newtonian fluid. In this section, we successively review the influence of gravity, the role of intermolecular forces, and the case of partial wetting. Other important deviations concerning high-velocity withdrawal (inertial effects) and the use of complex fluids as coating liquids (Marangoni coating) will be treated separately in Sections 4 and 5.

3.1 *Influence of Gravity*

Gravity has been neglected up to now, which is justified if the Laplace pressure is much larger than the hydrostatic one. It corresponds to the limit of a small Bond number, which compares gravity and capillary forces; for a fiber (or a tube), it is written as $\mathrm{Bo} = \rho g r^2/\gamma = r^2\kappa^2$ (with ρ the liquid density, g the gravity acceleration, and κ^{-1} the capillary length). The condition $\mathrm{Bo} \ll 1$ is

usually fulfilled up to radius of a fraction of a millimeter. For example, for a fiber of radius $r = 400\ \mu$m in a silicone oil, we get $\mathrm{Bo} = 0.07$.

When the Bond number (or its square root, often referred to as the Goucher number) is not negligible compared with unity, the film thickness depends on both the capillary and the Bond numbers (Tallmadge et al 1965). A particular case is the limit of an infinite fiber radius ($\mathrm{Bo} \to \infty$), which is clearly not described by Equation 7, where it implies an infinite thickness. In this case, which corresponds to the withdrawal of a plate, the characteristic length becomes the capillary length κ^{-1}, which is the typical size of the static meniscus of a wetting liquid along a vertical plate. Thus, r must be replaced by κ^{-1} in Equation 7; besides, the numerical coefficient changes from 1.34 to 0.94 (Derjaguin & Levi 1964) and the coating equation is written

$$h = 0.94\,\kappa^{-1}\mathrm{Ca}^{\frac{2}{3}} \tag{9}$$

which is the original form of the LLD equation.

The crossover from the fiber to the plate occurs around $\mathrm{Bo} = 1$ ($r = \kappa^{-1}$), as shown theoretically and experimentally by White and Tallmadge (1965b & 1966). Improvements in the theory were proposed by Wilson (1988). Similar studies were done for the drainage of capillary tubes of large inner radius (Lasseux & Quintard 1991).

In the plate case (Figure 1*a*), increasing the capillary number makes the film thicker (Equation 9), which thus becomes more and more sensitive to gravitational drainage. Hence for large capillary numbers, the surface tension should not play any role. Derjaguin suggested looking for a behavior of the form $h \sim \kappa^{-1}\mathrm{Ca}^{\mathrm{n}}$ independent of γ, which gives $\mathrm{n} = 1/2$ (Derjaguin & Levi 1964). In this visco-gravitational regime, the film is not flat but has a parabolic profile because of the gravitational drainage (Jeffreys 1930). The crossover from the capillary regime to the gravitational one is particularly large (6 orders of magnitude in capillary number), which makes the two asymptotic regimes difficult to study separately (White & Tallmadge 1965b).

3.2 *Role of the Intermolecular Forces*

At a very low velocity, the entrained film is so thin that intermolecular forces cannot be ignored (the range of van der Waals forces is of the order of 100 nm). When these forces favor a thick film, van der Waals forces are often described via a disjoining pressure $\Pi(h)$, which is the pressure that must be applied to the film surface to maintain it at a thickness h smaller than the range of the force (Derjaguin 1955). For nonretarded forces, it is written as $\Pi(h) = -\mathrm{A}/6\pi h^3$, where A is the Hamaker constant which is negative for most wetting films (Israelashvili 1985, de Gennes 1985). Because of the thickening effect of long-range forces, the film is expected to be thicker than predicted by Equation 7 and

to settle at a value independent of the capillary number (Teletzke et al 1988). The equilibrium thickness is determined by balancing the disjoining pressure with the capillary one (of order γ/r for thin films on fibers), which yields

$$h = a^{\frac{2}{3}} r^{\frac{1}{3}}, \tag{10}$$

where a is a microscopic length ($a = \sqrt{-A/6\pi\gamma}$), generally on the order of 1 Å. Thus, the equilibrium thickness is expected to be between 1 and 10 nm. Together with Equation 7, Equation 10 finally provides the capillary number below which the thickness should be a constant. It is written simply $Ca \sim a/r$, of order 10^{-5}–10^{-4} for fiber radii between 10 and 100 μm. Such a plateau was indeed observed for a very slow withdrawal out of a bath of wetting liquid (Quéré et al 1989). Effect of disjoining pressure on the film thickness was also investigated for films remaining inside a capillary tube by Derjaguin and Bondarenko, from which the Hamaker constant could be measured (Derjaguin et al 1972, Bondarenko et al 1977). All these different experiments require smooth solids, since the surface roughness would also be a natural cause of plateau in the limit of small thicknesses, as emphasized by Bretherton (1961) and shown experimentally by Chen (1986).

A closely related problem is the spontaneous formation of a microscopic wetting film on a fiber put in contact (i) with a liquid (Brochard 1986) or (ii) with a vapor likely to condense on the fiber (Gelfand & Lipowsky 1987, Upton et al 1989). The main feature is the effect of curvature, which fixes the film thickness as in Equation 10. Comparing the situation with a planar one, slight shifts for the threshold in spreading parameter (case i) or in wetting temperature (case ii) have also been theoretically predicted. The existence of such microscopic films was shown by di Meglio (1986), by depositing two drops close to each other on a fiber; after a while (corresponding to the progression of a microscopic film finally able to connect the drops), it could be observed that the smaller drop, of higher Laplace pressure, emptied in the larger one via this microscopic channel.

3.3 *The Dry Regimes*

When the solid is only partially wetted by the liquid, long-range forces generally squeeze the film (the disjoining pressure is negative). Hence one could expect that a transition would be observed as a function of the capillary number—no film below a threshold, then a sharp increase up to the thickness corresponding to the range of the intermolecular forces (typically 100 nm), and finally the LLD law (Teletzke et al 1988).

Such a transition between a dry and a wet regime indeed is observed (Petrov & Radoev 1981), but the critical thickness for which there is a sharp transition is found to be generally on the order of 1 μm, much larger than the range of

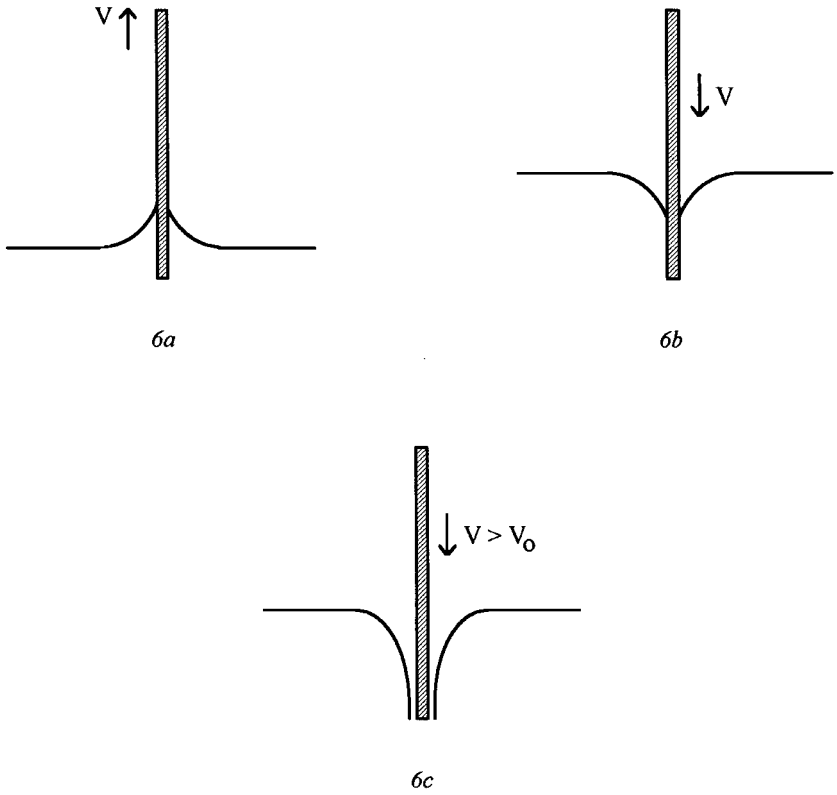

Figure 6 Dry regimes: (*a*) in partial wetting situations, a solid can come dry out of a bath if slowly drawn; (*b*) if plunging a solid quickly in a liquid bath, the dynamic contact angle is obtuse; (*c*) at still higher velocities, film of air can be entrained.

van der Waals forces (Quéré & Archer 1993). Actually, the dry regime involves a moving contact line (the line where the solid, the liquid, and the vapor coexist); the liquid wedge close to it is able to resist to viscous dissipation provided that the line velocity is not too high (de Gennes 1986) (Figure 6*a*). Above a threshold (typically about 1 cm/s), viscous forces dominate capillary ones. A film is left, and the LLD regime is recovered (Figure 1*d*). The critical velocity above which fluid coating occurs is mainly fixed by the material's properties (Sedev & Petrov 1992). In particular, it sharply increases with the static receding contact angle (Quéré & Archer 1993) but does not depend on the fiber curvature (Sedev & Petrov 1988, 1992).

Conversely, the fiber (or more generally the solid) can be dipped inside the bath (Figure 6*b*). By taking photographs, Inverarity (1969) measured the

dynamic contact angle between the liquid and a fiber at the entrance of the bath as a function of the velocity V (ranging between 10 μm/s and 10 m/s) and the liquid viscosity η (between 1 mPa $\cdot$ s and 1 Pa $\cdot$ s). The contact angle is found to be an increasing S-shaped function of ηV, from 0° (when the solid is wetted by the liquid) to 180°. These results were confirmed by Hoffman (1975), who showed by a series of measurements inside a capillary tube that the dynamic contact angle for a wetting liquid is a function only of the capillary number.

The problem of the dynamic contact angle has been widely covered since these pioneering studies but remains quite controversial (Dussan 1979, Blake 1993). Various angle-velocity relationships have been found experimentally (see for example Hayes & Ralston 1993 for a good summary); recent progress concerns the vicinity of the contact line where accurate descriptions of the shape of the meniscus have been reported (Dussan et al 1991, Shen & Ruth 1998). On the theoretical side, different approaches were proposed: (i) hydrodynamic models, where surface forces are balanced by viscous ones in the liquid wedge (Voinov 1976, de Gennes 1986, Cox 1986); (ii) molecular kinetic theory, involving molecular jumps close to the contact line (Blake & Haynes 1969, Blake 1988). [These approaches should be complementary; at low velocity, the hydrodynamic model seems adequate whereas molecular features should dominate at high speed (Brochard-Wyart & de Gennes 1992, Ruckenstein 1992, Petrov & Petrov 1992)]; (iii) numerical simulations, particularly interesting to investigate the boundary condition (i.e. the possibility of slip) in the microscopic vicinity of the contact line (Koplik et al 1988, Thomson & Robbins 1989, 1990).

As the dynamic angle approaches 180°, Inverarity (1969) observed that air entrainment can occur at the entrance of the bath (Figure 6*c*). The criteria for making a film of air at the entrance of a bath have been investigated by several authors (Blake & Ruschak 1979, Burley & Kennedy 1976, Burley et al 1984, Ghannam & Esmail 1990), often by plunging tapes into a bath. Similar studies were also performed with fibers by Ghannam & Esmail (1993), who show that the results are independent of the fiber radius. In each case, the critical velocity V_o above which air entrainment occurs was measured. Some interesting correlations were obtained (for example, the higher the viscosity, the lower the threshold), but there are no general laws; for example, the role of the static advancing angle was not clearly investigated; otherwise, measurements of the thickness of the film of air (which is highly unstable) are missing. In practice, a full understanding of the laws of air entrainment would be very useful; the critical velocity V_o is often a limit in coating processes because air entrainment at the entrance of the bath can be the cause of an irregular coating or even of no coating at all if the time spent by the solid in the bath is on the order of the lifetime of the air film.

4. QUICK COATINGS: INERTIAL EFFECTS

Even for large capillary numbers (Equation 8), we have supposed small coating velocities, which can be practically achieved with very viscous oils, as in Figure 5. We now describe the coating with a liquid of low viscosity, for which the condition of a small capillary number can be fulfilled even at large velocity: coating with water at $\mathrm{Ca} = 0.01$ implies a velocity on the order of 1 m/s, much larger than considered up to now. Then inertia, which was neglected (in Equation 3) to derive the LLD law, may become important. The Weber number evaluates its influence by comparing inertia with capillary force. It is written as

$$\mathrm{We} = \frac{\rho \mathrm{V}^2 r}{\gamma} \tag{11}$$

where ρ is the liquid density. (Alternatively, a Reynolds number could also be introduced, as suggested by Tallmadge and Soroka (1969); taking as a characteristic length the fiber radius, this is written as $\mathrm{Re} = \rho r \mathrm{V}/\eta$, and thus is simply We/Ca.)

For a thin fiber (of radius 10–100 μm) coated with usual liquids, a small Weber number means withdrawal velocities smaller than 1 m/s; for a liquid of low viscosity, this condition also implies a small capillary number. To evaluate the influence of inertia in plate coating, the dynamic pressure, $\sim \rho \mathrm{V}^2$, must be compared with a typical hydrostatic pressure in the dynamic meniscus, which is $\rho g \kappa^{-1}$. Hence the radius must be replaced by the capillary length in the definition of the Weber number. A negligible Weber number corresponds to withdrawal velocities $< \sqrt{g\kappa^{-1}}$ (typically on the order of 10–20 cm/s).

4.1 *The Viscoinertial Regime*

To understand the influence of inertia on fiber coating, liquids of low viscosity must be used. For water, for example ($\eta = 1$ mPa $\cdot$ s), varying the velocity between 1 cm/s and 1 m/s for a fiber of radius 50 μm increases the Weber number from 10^{-4} to 1, whereas the capillary number always remains much smaller than 1. The latter condition allows us to compare the observed behavior with the LLD law (Equation 7).

Then, as shown in Figure 7, inertia strongly affects the coating laws. The data were obtained by drawing thin wires ($r = 63.5$ μm and $r = 12.5$ μm) out of water at velocities ranging from 30 to 180 cm/s (de Ryck & Quéré 1996). The LLD law (Equation 7 or Equation 8) is pictured in full line.

For both wires, the film thickness can be fitted by the LLD equation only at low velocity. Above a threshold in capillary number, the film thickness sharply rises with the capillary number, since it increases about tenfold by simply doubling of the velocity. A diverging behavior was also encountered with viscous oils (Figure 5), but it was observed for a capillary number of order 1 (instead

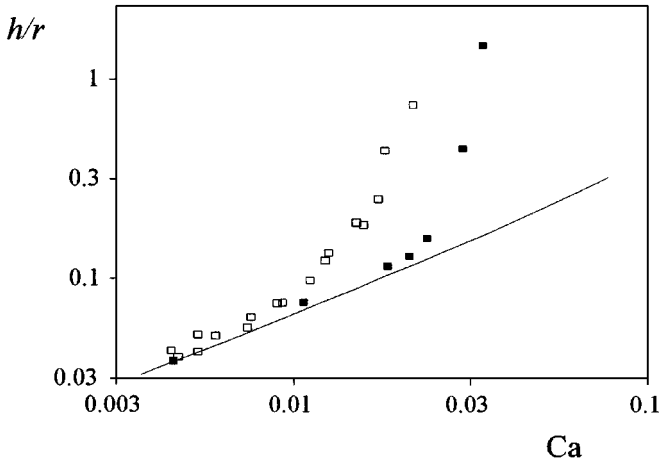

Figure 7 Quick coating out of water. The data quit the LLD and WT laws (Equations 7 and 8) above a threshold in velocity (typically 1 m/s) which depends on the fiber radius (black squares: $r = 12.5\ \mu$m; white squares: $r = 63.5\ \mu$m).

of 0.01 here) and had a smoother shape. The capillary number Ca^* for which the thickness diverges depends on the wire radius, because it roughly doubles when the radius is divided by 5. Thus, at large coating velocities, the capillary number is not sufficient for describing the data and a second dimensionless number must be introduced. Evaluated at the point where the thickness leaves the Landau law in Figure 7 (for $Ca \sim Ca^*$), the Weber number is found to be in both cases ~ 1, which confirms that inertia is responsible for the observed effect.

The reason inertia sharply thickens the film can be understood by considering Figure 4. The liquid enters the dynamic meniscus at a velocity of order V, and there undergoes a gradient of Laplace pressure. If the fluid kinetic energy per unit volume is larger than the capillary pressure, the latter can be neglected, and nothing retains the liquid any longer; the thickness diverges. The Weber number compares these two quantities, and thus a Weber number of unity provides the velocity V^* for which the divergence occurs. From Equation 11, we find

$$V^* \sim \left(\frac{\gamma}{\rho r}\right)^{\frac{1}{2}} \tag{12}$$

V^* varies slowly with the different parameters it contains and is generally ~ 1 m/s, which corresponds to a critical capillary number of 0.01 for pure water. Equation 12 also explains the dependence on wire radius observed in Figure 7 ($Ca^* \sim 1/\sqrt{r}$).

To have a feeling on the shape of the divergence, we can write dimensionally the Navier-Stokes equation:

$$-\frac{\rho V^2}{\lambda} + \frac{1}{\lambda}\frac{\gamma}{r} \sim \frac{\eta V}{h^2}, \tag{13}$$

which is Equation 3 written with the convective term. The Laplace pressure gradient and the convective term are of opposite signs, as explained above. Thus, the effective pressure in the film is written $p = \gamma/r - \rho V^2$, from which the length λ of the dynamic meniscus can also be evaluated. The matching is then shown as (still supposing $h \ll r$):

$$\frac{\gamma}{r} - \frac{\gamma h}{\lambda^2} \sim \rho V^2. \tag{14}$$

Putting together Equations 13 and 14 yields an expression for the thickness, as a function of both the capillary and the Weber numbers:

$$h \sim \frac{r Ca^{\frac{2}{3}}}{1 - We}, \tag{15}$$

where the numerator is the LLD thickness (Equation 6a). The denominator in Equation 15 appears to be the simplest factor making the thickness diverge for $We = 1$. This first-order analysis clearly emphasizes the parameters responsible for the divergence and appears to be in agreement with the data (de Ryck & Quéré 1996). On the base of a model proposed by Esmail & Hummel (1975), detailed calculations have been done, in quantitative agreement with the experiments (de Ryck & Quéré 1993b, Koulago et al 1995).

This regime of viscoinertial divergence can be observed if it occurs at a capillary number <1, the value for which a smooth capillary divergence takes place (see Equation 8). Together with Equation 12, it provides a condition for observing this regime. Written on the viscosity, it reads $\eta < \sqrt{\gamma\rho r}$. For standard values of the parameters, it implies a viscosity smaller than 40 mPa · s, a condition fulfilled in most practical situations where aqueous solutions are used.

Another question is whether the divergence could be also observed in plate coating experiments. On this point, the situation is rather confused since some papers predict that the effect of inertia should be to make the film thinner (and not thicker as observed) (Soroka & Tallmadge 1971, Esmail & Hummel 1975). Unfortunately, experimental data concerning high coating velocities were obtained with viscous oils, enlarging both the capillary and the Weber numbers (Spiers et al 1974), possibly with non-Newtonian effects (Gutfinger & Tallmadge 1965). In such conditions, calculations are hard to achieve. Recent numerical results, obtained from the case in which the capillary number

remains smaller than unity while the Weber number becomes nearly unity, exhibit a smooth divergence (de Ryck & Quéré 1998)—smoother than in the fiber case because of gravity, which makes the liquid flow down and thus limits the thickness. To the best of our knowledge, there is only one experiment corresponding to these conditions on We and Ca (Tallmadge & Stella 1968). For quick coating of a plate by pure water, a sharp increase of the film thickness above a threshold in velocity is indeed reported at small capillary number ($\mathrm{Ca} < 10^{-3}$).

4.2 *Entrainment of a Viscous Boundary Layer*

We now examine the coating at higher velocities. When the solid passes through the reservoir, the liquid close to it is put in motion because of the liquid viscosity. The layer entrained in volume is the viscous boundary layer, of thickness δ dimensionally given by balancing the acceleration of the fluid (of order $\rho \mathrm{V}/t$, where t is the contact time of the solid with the liquid) with the viscous force (of order $\eta \mathrm{V}/\delta^2$). Thus, we find at the exit of the reservoir (of length L):

$$\delta \sim \sqrt{\frac{\eta \mathrm{L}}{\rho \mathrm{V}}}. \tag{16}$$

At low velocity, δ is large compared with the thickness of the entrained film, given by Equations 7, 8, or even 15, and the arguments proposed above can be used. But if the Weber number is larger than 1, the regime is purely inertial (the capillary suction can be neglected), so that the film which comes out with the solid is the film that the solid has entrained in the volume, i.e. the viscous boundary layer. Then, we expect the film thickness to be simply given by Equation 16.

The proof that the high-velocity regime is unstationary is given by allowing the reservoir to be emptied by the running wire (de Ryck & Quéré 1994). In Figure 8, the mass of the reservoir is plotted versus time for a fiber ($r = 110\ \mu$m) drawn at $\mathrm{V} = 1.6$ m/s out of a bath of water of initial length $\mathrm{L}_o = 5.1$ cm (at point A, the wire is entrained; at point B, the reservoir is empty). The corresponding Weber number is 6, which implies a purely inertial regime.

The curve $m(t)$ is not linear but rather looks like a parabola. This shape is in agreement with the arguments exposed above: as time goes on, the reservoir gets shorter and the film thinner. If h is given by Equation 16, we have $h \sim \sqrt{\mathrm{L}}$. Together with $\mathrm{dL}/\mathrm{d}t \sim \mathrm{d}m/\mathrm{d}t \sim -h$ (for $h \ll r$), it yields $m \sim \mathrm{L} \sim t^2$, as observed in Figure 8.

Conversely, for a given length, the entrained thickness can be deduced from a slope measurement in Figure 8. It is plotted in Figure 9 versus the velocity for two reservoir lengths. After a slow and a quick increasing (respectively, the LLD and the visco-inertial regimes), the thickness indeed decreases with the

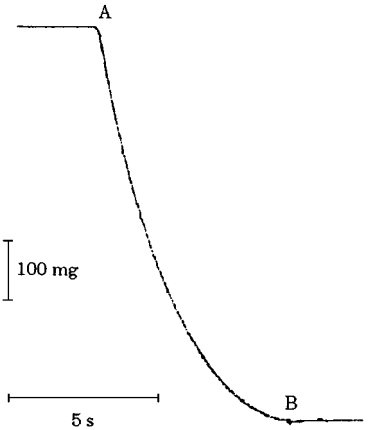

Figure 8 Mass of the reservoir when emptied by a moving wire at high speed (here 2 m/s). The entrainment is not stationary.

velocity, according to Equation 16 (drawn in full line). The fit provides a constant numerical coefficient in Equation 16 of 1.2 (± 0.1). Detailed calculations remain to be done to understand this value and to describe the transition between the divergence and the viscous boundary regime. In recent experiments done with pure water on the industrial device pictured in Figure 2, the viscous

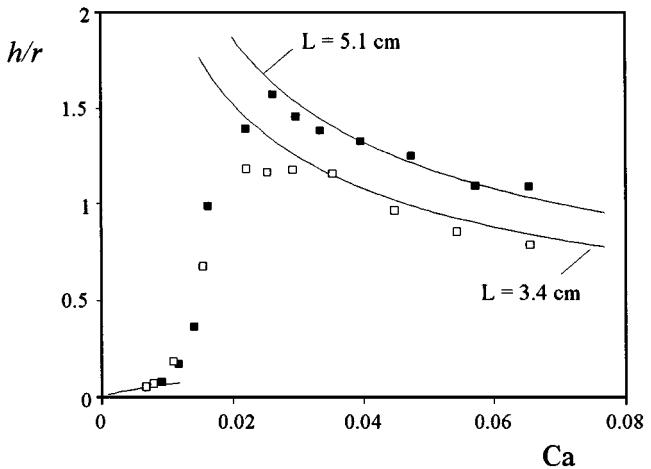

Figure 9 Summary of the different inertial regimes. Beyond the LLD regime (in full line, close to the origin) the film thickness first diverges; then it slowly decreases with the coating velocity. It follows Equation 16 (in full line) and depends on the length L of the reservoir.

boundary regime ($h \sim 1/\sqrt{\mathrm{V}}$) was shown to be valid at least up to 30 m/s (Huguet et al 1997).

Inertia finally appears to play two antagonist roles, as summarized in Figure 9: first, at intermediate speed (typically around 1 m/s), the inertia of the fluid moving close to the fiber thickens the film; then inertia of the immobile bath makes the film thinner. The film thickness is finally given by the smallest value between Equations 15 and 16. If the dipping time $\tau_{\mathrm{i}} = \mathrm{L}/\mathrm{V}$ is chosen as a control parameter, a similar nonmonotonous behavior is expected—first a parabolic increasing function (Equation 16); then, above $\tau_{\mathrm{i}}^* = \mathrm{L}/\mathrm{V}^*$ (see Equation 12), a decreasing of the film thickness. Such a behavior was also reported in freeze coating processes (where a cold wire is drawn from a hot molten phase), even if the problem is complicated in this case by the growth of a solid phase onto the wire surface, as stressed in the introduction.

4.3 *Expulsion of Droplets*

A third effect related to inertia can be observed if working with a long reservoir of small aperture (de Ryck & Quéré 1996). Figure 10 shows what happens with a reservoir of water about 10 times longer (initial length $\mathrm{L} = 30$ cm). At point A, a nickel wire ($r = 88.5$ μm) is moved at $\mathrm{V} = 0.5$ m/s.

Between A and B, the curve $m(t)$ has a stairs shape. Each step corresponds to the visible expulsion of a drop of radius R, the aperture of the reservoir. Between two stairs, the mass is not a constant but slowly decreases because the wire continuously entrains a film. After B, the expulsions stop.

The expulsion of droplets is caused by the impact of the viscous boundary layer on the outside meniscus of the bath. The capillary force retaining the

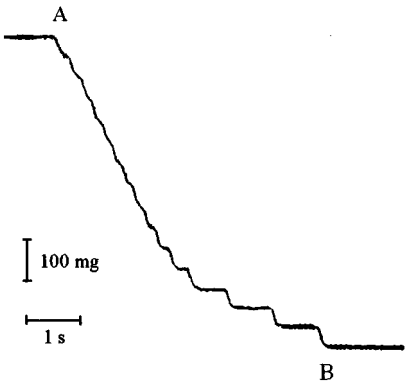

Figure 10 Quick coating out of a long reservoir. Its mass is plotted versus time. Drops are expelled, until point B.

meniscus and anchoring the drop inside the horizontal tube is γR, while the viscous force is the dynamic pressure (ρV^2) times the surface on which it applies, δ^2 (L is large, and we have $\delta \gg r$), where δ is given by Equation 16. Hence the viscous force is written simply: ηVL. If it exceeds the capillary force, the meniscus twists (as an umbrella in the wind) and a drop is removed. Equating these two forces gives the threshold of the expulsion regime, shown as

$$LCa \sim R. \tag{17}$$

For a given velocity V and aperture R, the drop expulsion occurs if the reservoir is longer than $L^* = R/Ca$. If a long reservoir is emptied by drawing a fiber out of it, first drops are expelled up to the point where L(t) reaches L^* (point B in Figure 10). Determined as a function of the velocity for different liquids, L^* was found to be in good agreement with Equation 17 (de Ryck & Quéré 1996). The characterization of this regime is practically important since drop expulsion is noxious for achieving a well-controlled regular coating.

5. COMPLEX FLUIDS

5.1 *Coating from a Soapy Water: the Thickening Effect*

Even a child knows that a film of water can be made in the absence of a solid: when blowing a bubble, a film of (soapy) water is sustained in air. Thus, in the presence of surfactants, the liquid-air interface has an ability of towing matter, like a solid-liquid interface. If a solid is drawn out of a bath containing surfactants, both the solid and the free interface can entrain matter, and the film is expected to be thicker than predicted for a pure liquid of the same characteristics.

This effect is indeed observed, as first reported by Carroll and Lucassen (1973). In their experiment, a textile fiber was pulled through an oil-water interface where surfactants were present. The thickness was deduced from a gravimetric analysis, after dissolution of the film in a solvent. For Ca varying from 2×10^{-3} to 10^{-1}, they showed that the presence of surfactants thickens the film by a factor of $\sim$2.5.

The simplest analysis of this thickening effect consists in supposing that the free interface moves at the same velocity as the solid. Such an assumption is classical in the closely related problem of the making of a soap film by moving a frame out of a solution of soapy water. Then it is supposed that the film surfaces go at the same velocity as the frame (rigid interface), which leads to Frankel's law for the soap film thickness (Mysels et al 1959):

$$h = 1.88\,\kappa^{-1}\,Ca^{\frac{2}{3}}, \tag{18}$$

which is the LLD law (Equation 9) for *two* plates (one per surface) drawn out of liquid. Mysels & Cox (1962) and Lyklema et al (1965) have confirmed Frankel's

law for solutions that provide a rigid interface, under the usual condition $Ca \ll 1$ and for films thick enough to neglect the effect of long range forces ($h > 100$ nm).

For fluid coating on a solid, supposing a rigid free interface implies that the film thickness still follows the LLD law at low speed ($h \sim Ca^{2/3}$) but modifies the numerical coefficient. Ratulowski & Chang (1990) and Park (1991) have shown that the thickening factor α (ratio of the actual thickness on the LLD one) is equal to

$$\alpha = 4^{\frac{2}{3}}, \tag{19}$$

which is 2.52, in close agreement with Carroll's experimental results (Carroll & Lucassen 1973).

Equation 19 is asymptotic, since the liquid-air interface cannot move faster than the solid; $4^{2/3}$ is the maximum thickening factor, and each value between 1 and $4^{2/3}$ should be observed. In Figure 11 for example, the film thickness is displayed versus the capillary number, for wire coating ($r = 88.5$ μm) out of a solution of SDS (sodium dodecyl sulfate) at a concentration of 20 g/L (about 8 times the critical micellar concentration) (Quéré et al 1997).

In this example, the thickening factor is found to be 1.8 (± 0.1), smaller than its predicted maximum of $4^{2/3}$ (Equation 19). Besides, it is independent of the drawing velocity, except for quick withdrawal ($Ca > 0.02$), where the beginning

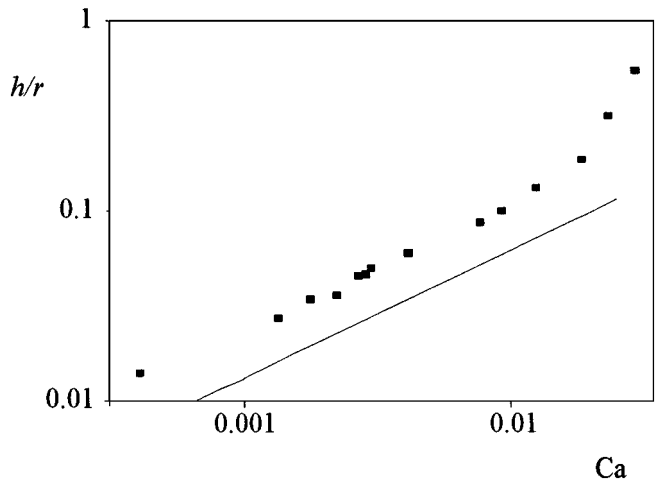

Figure 11 Coating a wire out of a solution of surfactant. At low velocity, all the data are above the LLD law (in full line); the film is thicker by a factor of order 2; at larger velocity, the beginning of the inertial regime can be observed.

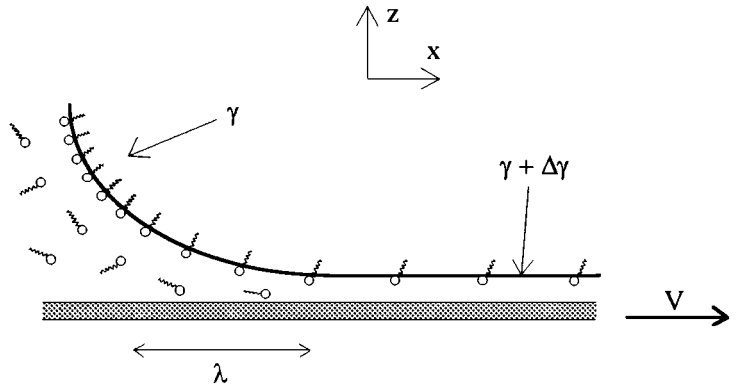

Figure 12 Drawing a solid out of a solution of surfactants can generate a gradient of concentration (and thus of surface tension) at the free surface.

of the divergence caused by inertia can be observed. Our aim is to understand what fixes the value of α and why it is independent of the velocity.

We first try to understand the reason the film is thicker than in the absence of surfactant (Carroll & Lucassen 1973, Ratulowski & Chang 1990, Park 1991). When drawing the solid, a gradient of surface concentration (and thus of surface tension) takes place in the dynamic meniscus, the region where the film forms (Figure 12). It is not an equilibrium situation. A so-called Marangoni flow sets up between the reservoir, of low surface tension γ, and the film of higher surface tension $\gamma + \Delta\gamma$, which causes the thickening of the film. This raises a delicate question since we need to know the actual value of the surface tension which holds in the dynamic meniscus to be able to calculate the capillary number (and then the thickening factor). In Figure 11, for example, the equilibrium surface tension was taken to calculate Ca.

To measure the surface tension in situ, we can take advantage of the diverging behavior caused by inertia. Since the thickness diverges when the Laplace pressure is similar to the dynamic pressure, the location of the divergence in Figure 11 gives access to the value of the surface tension at the exit of the dynamic meniscus (Equation 12). It is found that the divergence location can be understood only if a value very close to the equilibrium one is taken for the surfactant solution (Quéré et al 1997).

Thus, the tension difference $\Delta\gamma$ is much smaller than the tension γ itself. It can be understood by a simple argument (Ratulowski & Chang 1990). Before the detail of the velocity profile inside the dynamic meniscus can be found, two boundary conditions must be written. Very generally, there is no slippage at the solid-liquid interface, so that the velocity of the liquid at that boundary is the

solid velocity. This condition is responsible for liquid entrainment, in any case. At the liquid-air interface, the viscous stress, which is zero for a pure liquid, can be balanced by a surface tension gradient when surfactants are present. If x and z are the directions parallel and perpendicular to the flow (Figure 12), this condition is written

$$\eta \frac{\partial u}{\partial z}\bigg|_{surface} = \frac{d\gamma}{dx}, \tag{20}$$

where u is the fluid velocity along x. The experimental results justify the utilization of the LLD scaling for the characteristic lengths (Equation 6), so that Equation 20 dimensionally reads

$$\frac{\Delta\gamma}{\gamma} \sim Ca^{\frac{2}{3}}. \tag{21}$$

Thus, for small capillary numbers ($Ca \ll 1$), the surface tension difference is found to be much smaller than the surface tension itself ($\Delta\gamma \ll \gamma$), although it generates a strong thickening effect ($\Delta h \sim h$).

5.2 *The Thickening Factor*

A gradient of surface concentration of surfactants is responsible for the thickening effect. Diffusion could erase this gradient but it is dominated by convection in the experiments (and in most coating processes). Otherwise, the effect is observed above the critical micellar concentration: a large reservoir of surfactants stands under the surface, and adsorption from the volume is another possible mechanism for opposing the gradient. The time τ_v spent by the surfactant in the dynamic meniscus (of length $\lambda \sim r Ca^{1/3}$, Equation 6b), or transit time, is $\simeq \lambda/V$, and thus is written

$$\tau_v \sim \frac{r\eta}{\gamma} \frac{1}{Ca^{\frac{2}{3}}}. \tag{22}$$

Drawing a thinner fiber from a given solution makes the transit time shorter. Adsorption has less time to take place so that the thickening effect should be larger. This hypothesis was confirmed by doing systematic experiments with different wires. If plotted versus the fiber radius (Figure 13), the thickening factor is found to decrease monotonously with r, while remaining smaller than its maximum predicted value $\alpha = 4^{2/3} \approx 2.5$ (Equation 19).

Thus adsorption plays a key role in the thickening process. The kinetics of adsorption can be described by taking a linear form for the surfactant flux Q (per unit length) from the volume to the surface: $Q = \nu^* c \Delta\Gamma / \Gamma_o$, where Γ_o is the equilibrium surface concentration, $\Delta\Gamma$ the shift from equilibrium, c the volume concentration, and ν^* an intrinsic velocity depending on the surfactant (Ginley

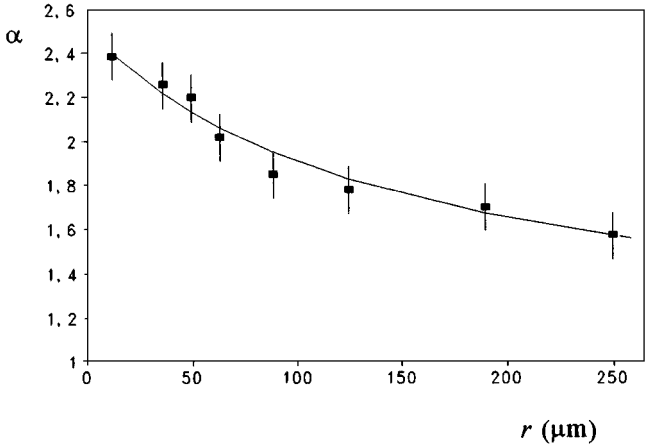

Figure 13 Thickening factor caused by the presence of surfactants in the bath as a function of the wire radius (for a given solution). The full line is Equation 24.

& Radke 1989). The surface concentration and the surface tension are related by the Marangoni number M ($M = -\Gamma/\gamma(\partial\gamma/\partial\Gamma)$). For small differences ($Ca \ll 1$, Equation 19), $\Delta\Gamma/\Gamma_o$ is simply proportional to $\Delta\gamma/\gamma$, the relative difference in surface tension across the dynamic meniscus.

The instantaneous adsorption time τ_{ad} related to this flux is $\tau_{ad} = \Gamma_o/Q$. Using Equation 21, its scaling with the different parameters is shown as

$$\tau_{ad} \sim \frac{M\Gamma_o}{\nu^* c} \frac{1}{Ca^{\frac{2}{3}}}. \tag{23}$$

It appears that τ_{ad} decreases with the velocity (the slower the withdrawal, the smaller the gradient and thus the smaller the adsorption flux) and in the same way as τ_v (see Equation 22). The ratio of these times is $\tau_{ad}/\tau_v = \mu/r$, where μ depends only on the liquid ($\mu = M\Gamma\gamma/\nu^* c\eta$ is typically 100 μm, thus $\sim r$). For any given solution and wire, the ratio τ_{ad}/τ_v is independent of V, which explains why the thickening is a constant as a function of the velocity (a result a priori paradoxical). The (dimensionless) thickening factor α is expected to be a function of the only (dimensionless) ratio, μ/r. The calculation can be done by balancing convection and adsorption. A simple interpolation function going from 1 to $4^{2/3}$ as μ/r goes from 0 to infinity is finally derived (Ou Ramdane & Quéré 1997):

$$\alpha \approx \left(\frac{4\mu + 2r}{\mu + 2r}\right)^{\frac{2}{3}}. \tag{24}$$

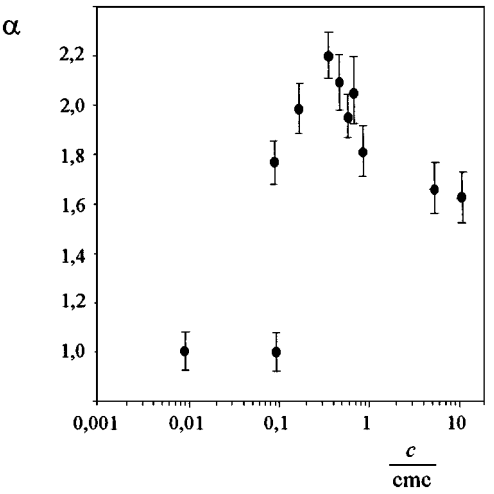

Figure 14 Thickening factor as a function of the surfactant concentration (for a given wire) (the cmc is the critical micellar concentration).

Equation 24 is illustrated in Figure 13 (full decreasing line) in good agreement with the data. The fit provides a value for μ ($\mu = 240$ μm), which finally yields $v^* \sim 1$ cm/s if taking $M = 1$. This velocity can be understood as the product of a velocity for crossing the interface times a Boltzmann factor since adsorption implies electrostatic and steric barriers. If V is the energy of the barrier and a and D the molecular size and diffusion constant of the surfactant, v^* should be computed as $v^* \sim D/a \exp(-V/kT)$, which would equal 1 cm/s if V is a few kT (with k the Boltzmann constant).

It is finally logical to be interested in the way the thickening factor depends on the surfactant concentration c (de Ryck and Quéré 1993a). This variation is displayed in Figure 14 for a nickel wire ($r = 63.5$ μm) drawn out of an SDS solution (the critical micellar concentration (cmc) is 8 mM).

Different features can be observed:

1. At a low concentration ($c < 1$ mM), there is no thickening. Experimental results can be hard to obtain in this regime because (i) the surfactant reservoir can gradually run out (Quéré & de Ryck 1998), and (ii) accidental contamination may occur. Nevertheless, it is clearly observed in Figure 14 that traces of contaminant do not generate any appreciable thickening, in contradiction with what is put forward to explain deviations to the LLD law in capillary tubes (Bretherton 1961, Ratulowski & Chang 1990, Park 1992). An important difference between the two geometries is the

existence in the tube of a point of accumulation at the top of the air bubble, where the surfactant can be concentrated.

2. For a concentration of about 0.1 cmc, the thickening effect suddenly appears; α sharply rises to a maximum ($\alpha = 2.2 \pm 0.1 < 4^{2/3}$) reached for $c \approx 0.4$ cmc. At this particular concentration, the curve $\gamma(c)$ (for the SDS) has an inflexion point; thus, $d\gamma/dc$ is maximum; this might be the reason the Marangoni flow is most efficient there.

3. Then the thickening slowly decreases with the concentration, in qualitative agreement with Equations 23 and 24: The larger the concentration, the quicker the adsorption. Quantitative comparison is hard to achieve because of the nontrivial dependence of τ_{ad} with c; it is not only inversely proportional to c, since Γ_o, M and ν^* should also depend on the concentration. In particular, above the cmc (where the thickening effect is still present), the way M and ν^* depend on c is not obvious.

4. For very concentrated systems (typically above 100 mM), the thickening effect does not remain independent of the capillary number. This case does not appear in Figure 14, where all the data correspond to a constant thickening factor versus Ca. It is observed that α slowly decreases with increasing Ca (Quéré & de Ryck 1998). Empirically, $h(\mathrm{Ca}) \sim \mathrm{Ca}^{1/2}$, which looks like behaviors predicted by Ratulowski & Chang (1990). Quantitative fits are not possible because Ratulowski's model is restricted to trace amounts of impurities. At still higher concentrations (above 300 mM), the data get very close to the LLD behavior ($\alpha \to 1$); an excess of surfactant kills the thickening effect. There is no theory for concentrated solutions which would allow us to understand quantitatively these observations.

As a conclusion, surfactants at intermediate concentrations provoke a thickening of the film, because of the Marangoni flow they induce in the dynamic meniscus. The film thickness is roughly doubled by the presence of surfactants, because each interface has the ability of entraining matter. In detail, the thickening factor depends on the surfactant concentration and the wire radius but surprisingly not on the drawing speed. These facts can be understood by balancing convection and adsorption of the impurities in the dynamic meniscus. Other regimes predicted by Ratulowski & Chang (1990) remain to be characterized. An extension of these results to the making of soap films (and bubbles) would be welcome.

5.3 *Emulsions*

What finally happens when drawing a solid out of an emulsion? This case was historically studied very early, since the LLD theory was developed to characterize the deposition of photographic light-sensitive emulsions on flexible solids (Derjaguin & Levi 1964). Although the LLD theory concerns Newtonian fluids, concentrated emulsions (or suspensions) are generally non-Newtonian and often behave as Bingham fluids: the force τ (per unit area) necessary to move two adjacent layers with a velocity gradient u_z is not simply proportional to u_z, but also implies a minimum force τ_o to put the liquid in motion (τ_o is the so-called yield stress). Thus, τ writes:

$$\tau = \tau_o + \eta u_z. \tag{25}$$

More generally, the coefficient η may itself depend on the shear rate u_z. A survey on this kind of viscoplastic fluid can be found in Bird et al (1982).

The calculation for the entrainment of a Bingham fluid is hard to achieve, but an interesting limit pointed out by Derjaguin & Levi (1964) is the case in which the term proportional to the velocity gradient can be ignored in Equation 25. Then the dynamic meniscus is the place of plastic deformations, and the viscous stress attains its limiting value τ_o in the vicinity of the solid surface. Neglecting gravity, the balance between the Laplace pressure and the viscous stress is dimensionally written (instead of Equation 3, for a Newtonian fluid):

$$\frac{\tau_o}{h} \sim \frac{1}{\lambda}\frac{\gamma}{r}. \tag{26}$$

The length of the dynamic meniscus is still given by Equation 5. Thus, the film thickness follows the Derjaguin-Levi (DL) law:

$$h \sim \frac{\tau_o^2}{\gamma^2} r^3. \tag{27}$$

Like in the LLD theory, the numerical constant in Equation 27 can be calculated by an asymptotic matching: it is found to be $\sim$13.0 (Derjaguin & Levi 1964). The dimensionless number $B = (\tau_o r/\gamma)^2$ is generally negligible compared with unity (for $\tau_o = 1$ Pa, B is $\sim 10^{-6}$), a condition necessary for Equation 27 to be valid. Of course, Equation 27 can be generalized to other geometries, for example to plate withdrawal, by replacing the fiber radius by the capillary length; the numerical coefficient is affected in such a modification.

Equation 27 is independent of the withdrawal velocity, which is logical since the velocity gradient was neglected in Equation 25. Derjaguin's proposition for considering the effect of viscosity just consists in adding the LLD (Equation 7) and the DL (Equation 27) thicknesses. To the best of our knowledge, there is no

experimental evidence of the DL theory. For the fiber case, it should concern such unexpected situations as coating of eyelashes by mascara!

Another interesting case concerns the very dilute emulsions, for which there is no non-Newtonian effect. Among the questions that can be raised, we want to know whether the film has necessarily the same composition as the reservoir. When one empties a glass of milk, an opalescent film remains on the glass, which indicates that the film contains oil drops. The LLD law allows us to evaluate the film thickness; it is typically about 20 μm (taking 1 cm/s for the emptying velocity of the glass), which is large compared with the drop diameter Φ in an emulsion ($\Phi \sim 1$ μm).

In the other limit ($h < \Phi$), which concerns very slow coatings, it was found in preliminary experiments that the film is often enriched in oil (Quéré & de Ryck 1998). A model of capture was proposed to understand this effect. If we suppose that the solid entrains all the droplets present in its vicinity, the oil quantity is independent of the velocity, increases with the concentration, and exceeds at small velocity what would be predicted by the LLD law—as observed experimentally.

Of course, this result cannot be general. The capture can be promoted by attractive long-range interactions between the oil drops and the solid (through a layer of water), but repulsive interactions can also exist (if decreasing the oil or solid polarizability), so that the film could be impoverished in oil if compared with that in the reservoir. A detailed classification remains to be done but such an experiment could be a direct way to evaluate interactions of oil droplets with a solid (in a water environment), a subject for which results are rather contradictory. The role of the droplets' deformability can be also questioned: we can wonder what happens if the drop is not deformable (i.e. a suspension instead of an emulsion); for attraction, does the capture resist as in the shear in the dynamic meniscus? Finally, the regime of very high speed, where the same interesting limit ($h < \Phi$) is also reached, should be worth studying.

6. AFTER THE COATING

6.1 *The Plateau-Rayleigh Instability*

A fluid film on a fiber is generally unstable (Plateau-Rayleigh instability) (see for example Middleman 1995). Because of the liquid surface tension (Plateau 1873), it spontaneously undulates and finally breaks into a periodic array of droplets. Plateau showed that all the axisymmetric wavelengths larger than the circumference $2\pi(r+h)$ of the fluid cylinder are unstable. The selection of one unique wavelength is a dynamic process, as understood by Lord Rayleigh; among all the possible ones, the fastest mode predominates (Rayleigh 1892, Tomotika 1935). For thin films on fibers ($h \ll r$), the selected wavelength

(which often corresponds to the distance between droplets) is found to be $2\pi\sqrt{2}r$.

In the same limit ($h \ll r$), the characteristic time scale t_o of the instability is obtained by balancing capillary with viscous forces. It is found that t_o scales as $\eta r^4/\gamma h^3$, which can be very large because of the viscous resistance to flow. If the film thickness is given by the LLD law (Equation 7), t_o is written as $\gamma r/\eta V^2$. For a typical Landau velocity (let us say 1 cm/s), this time is much longer than the formation time of the film (given in Equation 22). The ratio between these two times is typically 10^5, which shows that the droplet and the film formations are completely decoupled. The dynamics of the instability can be different for thick films ($h \gg r$, which includes the particular case of liquid columns for which $r = 0$): for liquids of low viscosity, the viscous force can be neglected, and the characteristic growth time for the drops is obtained by balancing capillary forces and inertia, which yields $t \sim (\rho h^3/\gamma)^{1/2}$ (much smaller than t_o).

Goren (1962) measured the selected unstable wavelength by brushing honey onto metallic wires and taking photographs. The results were found to be in good agreement with the above predictions. He also plotted the shape of the undulating cylinder of fluid during the instability and successfully compared it with calculations (Goren 1963). He showed in particular that the film between two growing bumps is cylindrical, so that a satellite droplet can appear between the main ones. An accurate description of the formation of such satellite drops was proposed by Yarin et al (1993). The shape of the ultimate succession of drops and the coverage rate of the fibers were studied by Roe (1975).

Extensions of Goren's works to the case of non-Newtonian fluids were proposed by Dumbleton & Hermans (1970). Effect of the presence of a surfactant at the liquid-fluid interface, of practical importance in detergency, was studied by Carroll & Lucassen (1974): they found by theory and experiment that the growth of instability is slowed down by a factor of $\sim$4 (as compared with a clean interface), because of the resistance of the surface against deformations caused by the surfactant. The case of extremely thin films, for which the long-range forces cannot be neglected, was studied by Starov & Churaev (1978) and Brochard-Wyart (1986). For a positive disjoining pressure, the film should be stabilized if it is thin enough ($h < a^{1/2}r^{1/2}$), where a is defined in Equation 10; this microscopic length reflects the strength of the intermolecular forces.

For a thin viscous fluid inside a capillary tube, the same instability occurs. A description for the film evolution equation was proposed by Hammond (1983) who modeled the appearance and growth of periodically spaced lobes. Above a threshold in thickness (of $0.2r$), Gauglitz & Radke (1988) showed that lobes finally pinch off and form lenses across the tube, as confirmed experimentally by Aul & Olbricht (1990). In this limit of thick films, linear approximations break

down, which requires improved theoretical treatments (Newhouse & Pozrikidis 1992).

6.2 *Annular Films Flowing*

The films along a rod or a fiber are often flowing, for example because of gravity. Generated by a famous study by Kapitza (1965), the nonlinear theory of evolution of waves in a viscous layer was mainly developed by Shkadov (Esmail & Shkadov 1971, Shkadov 1977, Bunov et al 1984, Demekhin & Shkadov 1985). A remarkable point is that the flow can keep the film from rupturing in droplets (as it should because of the Plateau-Rayleigh instability), as shown by Frenkel et al (1987). This is owing to a non-linear saturation of the instability, generated by the coupling between the growth of the instability and the flow. Then the interface chaotically oscillates, with an amplitude smaller than the average film thickness (Shlang & Sivashinsky 1982) so that the film seems to be stabilized.

Quéré (1990) found experimentally the condition for observing the permanence of such a continuous macroscopic film on vertical fibers covered with a liquid: the film thickness must be smaller than r^3/κ^{-2} (where κ^{-1} is the capillary length), which corresponds to a growth time of the instability t_0 smaller than the convection time of liquid on a wavelength, a condition for saturation to take place. This criterion was confirmed by Frenkel (1992), and a complete quantitative theory including a numerical film evolution equation was finally proposed by Kalliadasis & Chang (1994).

A related interesting case concerns core-annular flows, i.e. oil flows lubricated with water in a pipe. A complete description of the flows generated in such a situation can be found in the review by Joseph et al (1997). A remarkable set of shapes for the oil-water interface (including a spectacular bamboo profile) is reported, according to the flow.

6.3 *Pearls and Drops*

The droplets that generally form on fibers are the reason it is commonly said that it is impossible to wet fibers. It must be emphasized that the cylindrical geometry makes possible that a droplet makes a zero-contact angle on the fiber without being spread—a noticeable difference with the planar case. A question of practical importance often raised is whether a (microscopic) film can remain between the drops (di Meglio 1986).

The shape of the drops is given by a pressure balance. In the absence of gravity (small Bond numbers), it is just written that the Laplace pressure must be a constant. Then drops can have an unduloidal shape that conserves the axisymmetry; on a wire, droplets look like pearls. Furthermore, in wetting situations (Figure 15), the profile has generally an inflection point since the drop must

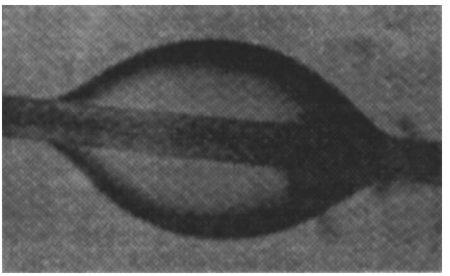

Figure 15 A wetting drop on a wire generally forms a pearl (conservation of axisymmetry) (from Carroll 1986).

join the fiber with a very small (possible zero) contact angle (MacHale et al 1997).

It is often of practical interest to measure the contact angle of liquids on fibers, and two broad classes of methods were developed: the Wilhelmy method and the drop shape analysis.

In the Wilhelmy method, the fiber is attached to a balance and partially immersed in a bath of liquid. The force acting on the fiber is recorded while slowly moving it (up and down), from which the static (receding and advancing) contact angles can be deduced (Miller 1985). Moving the fiber more quickly gives access to dynamic contact angles (Figures 6*a* & 6*b*).

Direct observations, which allow in-situ measurements, and drop shape analysis are also possible (Yamaki & Katayama 1975, Carroll 1976, Wagner 1991). For a given volume, measuring the length and height of the drop (and comparing them with computed values deduced from the Laplace equation) gives access to the contact angle, with an accuracy much better than obtained with a simple observation. An improvement of this technique consisting in digitalizing and calculating the whole profile of the drop was recently proposed by Song et al (1998).

Such observations were used to characterize the wetting of fibers in three practical situations. (i) The influence of surface roughness was studied by Carroll (1984), which is particularly useful to understand the wetting of natural fibers. Hairs for example exhibit a succession of scales (with a typical roughness of 0.5 μm) on which the contact line has the ability to hinge (Carroll 1990). (ii) Kumar & Hartland (1988 & 1990) extended the description to the case of drops on vertical fibers, for which gravity induces deformations, and in particular a difference between the upper and lower contact angles. (iii) Carroll studied the evolution of the contact angle in a detergency situation. A fiber coated with oil was put in an aqueous solution containing surfactants, and the

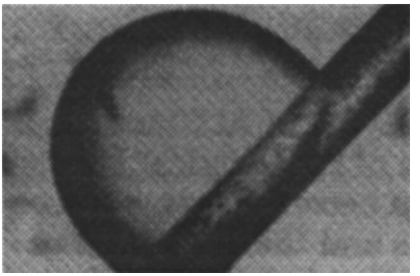

Figure 16 For a larger contact angle, the drop rolls on one side of the fiber (from Carroll 1986).

progressive dissolution of the oil was recorded photographically together with the evolution of the contact angle (Carroll 1981, Doyle 1991). Because of the presence of a surfactant, the contact angle (generally) increases with time, and drops get smaller (because of the dissolution). Then the drop can loose its axisymmetry; for minimizing its interfacial energy, it rolls on one side of the fiber (Figure 16). This process, first reported by Adam (1937) and called roll-up, is a fundamental step in detergency processes since it implies a reduction of the drop-fiber area. Carroll (1986) studied this transition experimentally and calculated the critical contact angle (depending on the fiber radius and drop volume) above which the axisymmetric configuration becomes metastable.

7. CONCLUSION

A simple question opened this review: what is the thickness of the film entrained by a solid, and more specifically by a fiber? Thanks to a series of experiments, we can now propose a classification (and in each class, an answer to the question), founded on the coating velocity.

1. At low velocity (corresponding to negligible Weber numbers) and if using a viscous oil, fluid coating obeys the LLD law (Equation 7), possibly corrected by White and Tallmadge (Equation 8) when the thickness approaches the fiber radius. This regime was referred to as visco-capillary, since the film thickness results from a balance between capillarity and viscosity. In the case of extremely slow coating, long-range forces must be taken into account: the film thickness becomes independent of the velocity (Equation 10).

Since low velocities correspond to thin films, it is logical that interfaces play a key role in this limit. The solid-liquid interface entrains matter because of the liquid viscosity, but the liquid-air interface can also do this if surfactants are present in the bath. Coating a solid from a surfactant solution provokes a thickening of the entrained film, if compared with coating from a pure liquid of the

same viscosity and surface tension. The effect is caused by the Marangoni flow that takes place when drawing the solid out of the solution, and the thickening factor lies between 1 and $4^{2/3}$. In most usual cases (concentrations between 1 and 100 mM), its value results from a balance between convection (which causes the thickening) and surfactant adsorption from the volume (which may erase the surface gradient).

For entrainment of an emulsion, the film can be enriched in oil because of the capture of oil droplets by the solid-liquid interface, if there is an attraction between the drops and the solid. As stressed above, coating with complex fluids is a world in itself and will need further studies to be fully understood, which is of practical importance, since most of the coating solutions are emulsions or suspensions.

2. At high velocity (typically above 1 m/s), measurements deviate tremendously from the Landau law, in spite of the capillary number remaining negligible compared with unity. Two successive regimes were discussed. First the film thickness sharply increases around a critical velocity V^* (Equation 12), and then slowly decreases for V much larger than V^*.

The diverging behavior was shown to happen when the Weber number We (Equation 11) becomes $\sim$1. It is caused by inertia and thus was called the visco-inertial regime. The kinetic energy of the fluid (per unit volume) increases with the velocity so that the fluid close to the solid becomes insensitive to the Laplace pressure, which tries to send it back to the reservoir: the thickness diverges (Equation 15). At larger velocities ($We > 1$), the viscous boundary layer is thin and limits the entrainment; the film thickness decreases as $1/\sqrt{V}$ and does not depend any longer on the surface tension (Equation 16). Practically, the viscous boundary layer regime should affect most industrial coating processes, where fibers or wires are lubricated at a velocity of 10–100 m/s.

If simple cases can be isolated, fluid coating still raises open problems. We mainly cite the case of non-Newtonian fluids, which are commonly used. These fluids are often heterogeneous, which is in itself a cause of eccentric behaviors (as shown in a very preliminary discussion on emulsions). This field should require further studies. It would be also worth trying to extend observations described here to other geometries, particularly to planar ones, where contradictory viewpoints coexist. The role of inertia is not clearly understood, and the making of soap films would require new experiments. As a final point, let us stress again that once a film is deposited on a fiber, the story is not finished; it undulates before breaking into a periodic array of droplets because of the liquid surface tension. In many cases where a regular coating is needed, the understanding of fluid coating must be coupled with a reflection on the way to stabilize it (generally by some drying or freezing mechanism). From this viewpoint, coating with a paste behaving as a Bingham fluid can be a solution,

by choosing a yield stress low enough to make possible the deposition but large enough to prevent the instability to develop. Such a situation would also deserve fundamental study—but we gradually leave *fluid* coating.

ACKNOWLEDGMENTS

This work summarizes 5 years of research. It could not have been achieved without all the students involved in the project: first, Alain de Ryck but also Élisabeth Archer, Olivier Ou Ramdane, Frédéric Restagno, Stéphanie Le Roux, and Anne-Sophie Huguet. We greatly benefited from innumerable discussions with Pierre-Gilles de Gennes, Françoise Brochard, Jean-Marc di Meglio, Alexander Koulago, Victor Shkadov, Hsueh-Chia Chang, and Manuel Velarde. Finally, the subject was constantly irrigated by the questions of our industrial partners: Pascal Chartier and Éric Dallies (Saint-Gobain), Michel Droux and Michel Arpin (Vetrotex), and Louis Vovelle (Rhône-Poulenc). It is a pleasure to thank all of them.

Literature Cited

Adam NK. 1937. Detergent action and its relation to wetting and emulsification. *J. Soc. Dyers Colour.* 53:122–29

Akter S, Hashmi MSJ. 1997. High speed nylon coating of wire using a plasto-hydrodynamic pressure unit. *J. Mat. Proc. Tech.* 63:453–57

Arridge RGC, Heywood D. 1967. The freeze coating of filaments. *Brit. J. Appl. Phys.* 18:447–57

Aul RA, Olbricht WL. 1990. Stability of a thin annular film in pressure-driven flow through a capillary. *J. Fluid Mech.* 215:585–99

Bird RB, Dai GC, Yarusso BJ. 1982. The rheology and flow of viscoplastic materials. *Rev. Chem. Eng.* 1:1–70

Blake TD. 1988. Wetting kinetics—How do wetting lines move? Presented at Annu. Meet. *Am. Inst. Chem. Eng.* on the mechanics of thin film coating, New Orleans, paper 1A

Blake TD. 1993. Dynamic contact angles and wetting kinetics. In *Wettability*, ed. JC Berg, p. 291–309. New York: Marcel Dekker

Blake TD, Haynes JM. 1969. Kinetics of liquid/liquid displacement. *J. Coll. Int. Sci.* 30:421–23

Blake TD, Ruschak KJ. 1979. A maximum speed of wetting. *Nature* 282:489–91

Bondarenko NF, Zheleznyi BV, Osipov YuA, Ostapenko NS. 1977. Rheological characteristics of thin wetting films of single-component liquids, as determined by a capillary method. *Koll. Z.* 39:241–51

Brelin JL, Kornmann M. 1990. Coating steel wires with copper and copper alloys. *Wire Ind.* 57:824–30

Bretherton FP. 1961. The motion of long bubbles in tubes. *J. Fluid Mech.* 10:166–88

Brochard F. 1986. Spreading of liquid drops on thin cylinders: The manchon/droplet transition. *J. Chem. Phys.* 84:4664–72

Brochard-Wyart F. 1986. Instabilité des films mouillant des fibres. *C.R. Acad. Sci. (Paris) II* 303:1077–80

Brochard-Wyart F, de Gennes PG. 1992. Dynamics of partial wetting. *Adv. Coll. Int. Sci.* 39:1–11

Bubnov MM, Dianov EM, Kazenin DA, Kutepov AM, Makeev AA, Semenov SL. 1994. On the application of a metallic coating on a fiber light guide. *Dokl. Chem. Tech.* 337:624–27

Bunov AV, Demekhin EA, Shkadov VYa. 1984. On the non-uniqueness of non-linear wave solution in a viscous layer. *Prikl. Matem. Mekhan.* 48:691–96

Burley R, Jolly RPS. 1984. Entrainment of air into liquids by a high speed continuous solid surface. *Chem. Eng. Sci.* 39:1357–72

Burley R, Kennedy BS. 1976. An experimental

study of air entrainment at a solid/liquid/gas interface. *Chem. Eng. Sci.* 31:901–11
Carreker RP. 1963. Dip-forming—a continuous casting process. *J. Metals* 15:774–80
Carroll BJ. 1976. The accurate measurement of contact angle, phase contact areas, drop volume, and Laplace excess pressure in drop-on-fiber systems. *J. Coll. Int. Sci.* 57:488–95
Carroll BJ. 1981. The kinetics of solubilization of nonpolar oils by nonionic surfactant solutions. *J. Coll. Int. Sci.* 79:126–35
Carroll BJ. 1984. The equilibrium of liquid drops on smooth and rough circular cylinders. *J. Coll. Int. Sci.* 97:195–200
Carroll BJ. 1986. Equilibrium conformations of liquid drops on thin cylinders under forces of capillarity. A theory for the roll-up process. *Langmuir* 2:248–50
Carroll BJ. 1990. Droplet formation and contact angles of liquids on mammalian hair fibers. *J. Chem. Soc. Faraday Trans.* 85:3853–60
Carroll BJ, Lucassen J. 1973. Capillarity-controlled entrainment of liquid by a thin cylindrical filament. *Chem. Eng. Sci.* 28:23–30
Carroll BJ, Lucassen J. 1974. Effect of surface dynamics on the process of droplet formation from supported and free liquid cylinders. *J. Chem. Soc. Faraday Trans.* 70:1228–39
Chen JD. 1986. Measuring the film thickness surrounding a bubble inside a capillary. *J. Colloid. Interface Sci.* 109:341–49
Cox BG. 1962. On driving a viscous fluid out of a tube. *J. Fluid Mech.* 14:81–96
Cox RG. 1986. The dynamics of the spreading of a liquid on a solid surface. *J. Fluid Mech.* 168:169–89
de Gennes PG. 1985. Wetting: statics and dynamics. *Rev. Mod. Phys.* 57:827–63
de Gennes PG. 1986. Deposition of Langmuir-Blodgett layers. *Coll. Polymer Sci.* 264:463–65
Demekhin EA, Shkadov VYa. 1985. Two dimensional wave regimes in a thin layer of a viscous fluid. *Izv. Akad. Nauk SSR, Mekh. Zhi. Gaz.* 3:63–67
Derjaguin BV. 1943. On the thickness of the liquid film adhering to the walls of a vessel after emptying. *Acta Physicochim. USSR* 20:349–52
Derjaguin BV. 1955. Definition of the concept of, and magnitude of the disjoining pressure and its role in the statics and kinetics of thin layers of liquids. *Colloid J.* 17:191–97
Derjaguin BV, Levi SM. 1964. *Film Coating Theory.* London: The Focal Press
Derjaguin BV, Zheleznyi BV, Tkachev AP. 1972. Effect of disjoining pressure on thickness of wetting film remaining on surface of cylindrical capillary after recession of liquid meniscus. *Dokl. Akad. Nauk USSR* 206:1146–49
de Ryck A, Quéré D. 1993a. Fibres tirées d'un bain. *C.R. Acad. Sci. (Paris) II* 316:1045–50
de Ryck A, Quéré D. 1993b. Entraînement visco-inertiel de liquide par un fil. *C.R. Acad. Sci. (Paris) II* 317:891–97
de Ryck A, Quéré D. 1994. Quick forced spreading. *Europhys. Lett.* 25:187–92
de Ryck A, Quéré D. 1996. Inertial coating of a fiber. *J. Fluid Mech.* 311:219–37
de Ryck A, Quéré D. 1998. Gravity and inertia effects in plate coating. *J. Coll. Int. Sci.* 203: 278–85
di Meglio JM. 1986. Mise en évidence d'un film mouillant sur des fibres textiles. *C.R. Acad. Sci. (Paris) II* 303:437–39
Doyle PJ. 1991. Formation and growth of water microdroplets in nonpolar oil-fiber-aqueous surfactant systems. *J. Coll. Int. Sci.* 143:195–204
Dumbleton JH, Hermans JJ. 1970. Capillary instability of a thin annular layer of liquid around a solid cylinder. *Ind. Eng. Chem. Fund.* 9:466–69
Dussan EB, V. 1979. On the spreading of liquids on solid surfaces: static and dynamic contact lines. *Annu. Rev. Fluid Mech.* 11:371–400
Dussan EB, V, Ramé E, Garoff S. 1991. On identifying the appropriate boundary conditions at a moving contact line: an experimental investigation. *J. Fluid Mech.* 230:97–116
Esmail NM, Hummel RL. 1975. Nonlinear theory of free coating onto a vertical surface. *A.I.Ch.E. J.* 21:958–65
Esmail NM, Shkadov VYa. 1971. Non linear theory of waves in a viscous liquid layer. *Izv. Akad. Nauk SSR, Mekh. Zhi. Gaz.* 4:54–59
Fairbrother F, Stubbs AE. 1935. The "bubble-tube" method of measurement. *J. Chem. Soc.* 1:527–29
Frenkel AL, Babchin AJ, Levich BG, Shlang T, Sivashinsky GI. 1987. Annular flows can keep unstable films from breakup: nonlinear saturation of capillary instability. *J. Coll. Int. Sci.* 115:225–33
Frenkel AL. 1992. Nonlinear theory of strongly undulating thin films flowing down vertical cylinders. *Europhys. Lett.* 18:583–88
Gatcombe EK. 1945. Lubrication characteristics of involute spur gears. *Trans. ASME* 67:177–88
Gauglitz PA, Radke CJ. 1988. An extended evolution equation for liquid film breakup in cylindrical capillaries. *Chem. Eng. Sci.* 43:1457–65
Gelfand MP, Lipowsky R. 1987. Wetting on cylinders and spheres. *Phys. Rev. B* 36:8725–35
Ghannam MT, Esmail NM. 1990. Effect of

substrate entry angle on air entrainment in liquid coating. *A.I.Ch.E. J.* 36:1283–86
Ghannam MT, Esmail NM. 1993. Experimental study of the wetting of fibres. *A.I.Ch.E. J.* 39:361–65
Ginley GM, Radke CJ. 1989. Influence of soluble surfactants on the flow of the long bubbles through a cylindrical capillary. *ACS Symp. Ser.* 396:480–501
Goren SL. 1962. The instability of an annular thread of fluid. *J. Fluid Mech.* 12:309–19
Goren SL. 1963. The shape of a thread of liquid undergoing break-up. *J. Coll. Sci.* 19:81–86
Goucher FS, Ward H. 1922. The thickness of liquid films formed on solid surfaces under dynamic condition. *Phil. Mag.* 44:1002–14
Groenveld P. 1970. High capillary number withdrawal from viscous newtonian liquids by flat plates. *Chem. Eng. Sci.* 25:33–40
Gutfinger C, Tallmadge JA. 1965. Films of non-Newtonian fluids adhering to flat plates. *A.I.Ch.E. J.* 11:403–12
Hammond P. 1983. Nonlinear adjustment of a thin annular film of viscous fluid surrounding a thread of another within a circular cylindrical pipe. *J. Fluid Mech.* 137:363–84
Hayes RA, Ralston J. 1993. Forced liquid movement on low energy surfaces. *J. Coll. Int. Sci.* 159:429–38
Hoffman RL. 1975. A study of the advancing interface. *J. Coll. Int. Sci.* 50:228–41
Huguet AS, Droux M, Arpin M, Quéré D. 1997. Unpublished results
Inverarity G. 1969. Dynamic wetting of glass fibre and polymer fibre. *Br. Polym. J.* 1:245–51
Israelashvili J. 1985. *Intermolecular and Surface Forces.* San Diego: Academic Press
James DF. 1974. The meniscus on the outside of a small circular cylinder. *J. Fluid Mech.* 63:657–64
Jeffreys H. 1930. The draining of a vertical plate. *Proc. Camb. Phil. Soc.* 26:204–05
Joseph DD, Bai R, Chen KP, Renardy YY. 1997. Core-annular flows. *Annu. Rev. Fluid Mech.* 29:65–90
Kalliadasis S, Chang HC. 1994. Drop formation during coating of vertical fibres. *J. Fluid Mech.* 261:135–68
Kapitza PL. 1965. *Collected papers (Vol. II),* p. 662–709. London: Pergamon Press
Koplik J, Banavar JR, Willemsen JF. 1988. Molecular dynamics of Poiseuille flow and dynamic contact lines. *Phys. Rev. Lett.* 60: 1285–88
Kornmann M, Rexer J, Anderson E. 1978. Aluminising process by high-speed hot dipping. *Wire Ind.* 6:322–25
Kornmann M, Talmor Y, Hirano S, Kambe R. 1983. High-speed, hot dipping of steel wire. *Wire J.* 8:52–58
Koulago A, Quéré D, De Ryck A, Shkadov V. 1995. Film entrained by a fiber quickly drawn out of a liquid bath. *Phys. Fluids* 7:1221–24
Kumar A, Hartland S. 1988. Shape of a drop on a vertical fiber. *J. Coll. Int. Sci.* 124:67–76
Kumar A, Hartland S. 1990. Measurement of contact angles from the shape of a drop on a vertical fiber. *J. Coll. Int. Sci.* 136:455–69
Lackey WJ, Hanigofsky JA, Groves MT, Heaney JA. 1991. Continuous fiber coating system. *Ceram. Eng. Sci. Proc.* 12:1048–63
Landau LD, Levich B. 1942. Dragging of a liquid by a moving plate. *Acta Physicochim. USSR* 17:42–54
Lasseux D, Quintard M. 1991. Épaisseur d'um film dynamique derrière un ménisque récessif. *C.R. Acad. Sci. (Paris) II* 313:1375–81
Levich VG. 1962. *Physical Hydrodynamics.* Englewood Cliffs: Prentice-Hall
Lyklema J, Scholten PC, Mysels KJ. 1965. Flow in thin liquid films. *J. Phys. Chem.* 69:116–23
Mac Hale G, Käb NA, Newton MI, Rowan SM. 1997. Wetting of a high-energy fiber surface. *J. Coll. Int. Sci.* 186:453–61
Middleman S. 1995. *Modeling Axisymmetric Flows.* San Diego: Academic Press
Miller B. 1985. Experimental aspects of fiber wetting and liquid movement between fibers. *Text. Sci. Technol.* 7:121–47
Morey FC. 1940. Thickness of a film adhering to a surface slowly withdrawn from the liquid. *J. Res. Natl. Bur. Stand.* 25:385–93
Mysels KJ, Cox MC. 1962. An experimental test of Frankel's law of film thickness. *J. Colloid Sci.* 17:136–45
Mysels KJ, Shinoda K, Frankel S. 1959. Soap Films. London: Pergamon Press
Newhouse LA, Pozrikidis C. 1992. The capillary instability of annular layers and liquid threads. *J. Fluid Mech.* 242:193–09
Ou Ramdane O, Quéré D. 1997. Thickening factor in Marangoni coating. *Langmuir* 13:2911–16
Park CW. 1991. Effects of insoluble surfactants on dip coating. *J. Coll. Int. Sci.* 146:382–94
Park CW. 1992. Influence of soluble surfactants on the motion of a finite bubble in a capillary tube. *Phys. Fluids A* 4:2335–47
Park CW, Homsy GM. 1984. Two-phase displacement in Hele-Shaw cells: theory. *J. Fluid Mech.* 139:291–308
Petrov JG, Radoev BP. 1981. Steady motion of the three phase contact line in model Langmuir-Blodgett systems. *Colloid. Polymer Sci.* 259:753–60
Petrov PG, Petrov JG. 1992. A combined molecular-hydrodynamic approach to wetting kinetics. *Langmuir* 8:1762–67

Plateau J. 1873. *Statique expérimentale et théorique des liquides soumis aux seules forces moléculaires*. Paris: Gauthier-Villars

Quéré D, Di Meglio JM, Brochard-Wyart F. 1989. Making van der Waals films on fibers. *Europhys. Lett.* 10:335–40

Quéré D. 1990. Thin films flowing on vertical fibers. *Europhys. Lett.* 13:721–26

Quéré D, Archer É. 1993. The trail of the drops. *Europhys. Lett.* 24:761–66

Quéré D, De Ryck A. 1998. Le mouillage dynamique d'une fibre. *Ann. Phys. (Paris)*, 23:1–154

Quéré D, De Ryck A, Ou Ramdane O. 1997. Liquid coating from a surfactant solution. *Europhys. Lett.* 37:305–10

Ratulowski J, Chang HC. 1990. Marangoni effects of trace impurities on the motion of long gas bubbles in capillaries. *J. Fluid Mech.* 210:303–28

Rayleigh Lord. 1892. On the instability of a cylinder of viscous liquid under capillary force. *Phil. Mag.* 34:145–207

Reinelt DA, Saffman PG. 1985. The penetration of a finger into a viscous fluid in a channel and tube. *SIAM J. Sci. Sta. Comput.* 6:542–61

Roe RJ. 1975. Wetting of thin wires and fibers by a liquid film. *J. Coll. Int. Sci.* 50:70–79

Ruckenstein E. 1992. Dynamics of partial wetting. *Langmuir* 8:3038–39

Ruschak KJ. 1985. Coating flows. *Annu. Rev. Fluid Mech.* 17:65–89

Schwartz LW, Princen HM, Kiss AD. 1986. On the motion of bubbles in capillary tubes. *J. Fluid Mech.* 172:259–75

Sedev RV, Petrov JG. 1988. Influence of geometry of the three-phase system on the maximum speed of wetting. *Colloids Surf.* 34:197–201

Sedev RV, Petrov JG. 1992. Influence of geometry on steady dewetting kinetics. *Colloids Surf.* 62:141–51

Shen C, Ruth DW. 1998. Experimental and numerical investigations of the interface profile close to a moving contact line. *Phys. Fluids* 10:789–99

Shkadov VYa. 1977. Solitary waves in a layer of viscous liquid. *Izv. Akad. Nauk SSR, Mekh. Zhi. Gaz.* 1:63–66

Shlang T, Sivashinsky GI. 1982. Irregular flow of a liquid film down a vertical column. *J. Phys.* 43:459–66

Song B, Bismarck A, Tahhan R, Springer J. 1988. A generalized drop length-height method for determination of contact angle in drop-on-fiber systems. *J. Coll. Int. Sci.* 197:68–77

Soroka AJ, Tallmadge JA. 1971. A test of the inertial theory for plate withdrawal. *A.I.Ch.E. J.* 17:505–08

Spiers RP, Subbaraman CV, Wilkinson WL. 1974. Free coating of a liquid onto a vertical surface. *Chem. Eng. Sci.* 29:389–96

Starov VM, Churaev NV. 1978. Thickness and stability of liquid films on nonplanar surfaces. *Koll. Zh.* 40:909–14

Tabeling P, Libchaber A. 1986. Film draining and the Saffman-Taylor problem. *Phys. Rev. A* 33:794–96

Tabeling P, Zocchi G, Libchaber A. 1987. An experimental study of the Saffman-Taylor instability. *J. Fluid Mech.* 177:67–82

Tallmadge JA, Labine RA, Wood BH. 1965. Films adhering to large wires upon withdrawal from liquid baths. *IEC Fundam.* 4:400–06

Tallmadge JA, Soroka AJ. 1969. The additional parameter in withdrawal. *Chem. Eng. Sci.* 24:377–83

Tallmadge JA, Stella R. 1968. Some properties of the apparent water paradox in entrainment. *A.I.Ch.E. J.* 14:838–40

Taylor GI. 1960. Deposition of a viscous fluid on a plane surface. *J. Fluid Mech.* 9:218–24

Taylor GI. 1961. Deposition of viscous fluid on the wall of a tube. *J. Fluid Mech.* 10:161–65

Taylor GI. 1963. Cavitation of a viscous fluid in narrow passages. *J. Fluid Mech.* 16:595–619

Teletzke G, Davis HT, Scriven LE. 1988. Wetting hydrodynamics. *Rev. Phys. Appl.* 23:989–1007

Thomson PA, Robbins MO. 1989. Simulations of contact-line motion: slip and the dynamic contact angle. *Phys. Rev. Lett.* 63:766–79

Thomson PA, Robbins MO. 1990. Shear flows near solids: epitaxial order and flow boundary conditions. *Phys. Rev. A* 41:6830–37

Tomotika S. 1935. On the instability of a cylindrical thread of a viscous liquid surrounded by another viscous fluid. *Proc. Roy. Soc. (London) A* 153:322–37

Upton PJ, Indekeu JO, Yeomans JM. 1989. Wetting on spherical and cylindrical surfaces: Global phase diagrams. *Phys. Rev. B* 40:666–79

Vaillant P. 1913. Sur un procédé de mesure des grandes résistances polarisables et son application à la mesure de la résistance de bulles dans un liquide. *C. R. Acad. Sci. (Paris)* 156:307–10

Voinov OV. 1976. Hydrodynamics of wetting. *Fluid Dyn.* 11:714–21

Wagner HD. 1991. Spreading of liquid droplets on cylindrical surfaces: accurate determination of contact angle. *J. Appl. Phys.* 70:493–96

White DA, Tallmadge JA. 1965a. Static menisci on the outside of cylinders. *J. Fluid Mech.* 23:325–35

White DA, Tallmadge JA. 1965b. Theory of

drag out of liquids on flat plates. *Chem. Eng. Sci.* 20:33–37
White DA, Tallmadge JA. 1966. A theory of withdrawal of cylinders from liquid baths. *A.I.Ch.E. J.* 12:333–39
White DA, Tallmadge JA. 1967. A gravity corrected theory for cylinder withdrawal. *A.I.Ch.E. J.* 13:745–50
Wilson SDR. 1988. Coating flows on to rods and wires. *A.I.Ch.E. J.* 34:1732–35
Xiao L, Li D, Wang S. 1994. Vertical hot dip aluminium coating of steel wire. *Wire Ind.* 61:639–44
Yamaki J, Katayama Y. 1975. New method of determining contact angle between monofilament and liquid. *J. Appl. Polym. Sci.* 19: 2897–909
Yarin AL, Oron A, Rosenau P. 1993. Capillary instability of thin liquid film on a cylinder. *Phys. Fluids A* 5:91–98

Annual Review of Fluid Mechanics
Volume 31, 1999

CONTENTS